

Improving color rendering index of WLEDs with convex-dual-layer remote phosphor geometry using red-emitting $\text{CaGa}_2\text{S}_4:\text{Mn}^{2+}$ phosphor

Nguyen Thi Phuong Loan¹, Anh Tuan Le²

¹Faculty of Fundamental 2, Posts and Telecommunications Institute of Technology, Vietnam

²Faculty of Electrical and Electronics Engineering, Ton Duc Thang University, Vietnam

Article Info

Article history:

Received Oct 2, 2019

Revised Apr 9, 2020

Accepted May 14, 2020

Keywords:

$\text{CaGa}_2\text{S}_4:\text{Mn}^{2+}$

Color rendering index

Dual-layer remote phosphor geometry

Mie-scattering theory

WLEDs

ABSTRACT

The white-light light-emitting diode (LED), a conventional illumination solution, usually consists of one chip and one phosphor layer, which leads to the insufficient color rendering index (CRI) in this configuration. To optimize the efficiency of WLED, a new LED package with 2 chips and one phosphor was proposed, this innovative configuration can yield more lights and achieve high CRI. Thus, this study aims at perfecting the color performance with the two chips and dual phosphor layers package with the proportions and densities of phosphor in the silicone constantly changed to find the best option. The white-light LED module is adjusted using a specialized color design model. The comparison results between the measured and the simulation from the color design model CIE 1931 color coordinates suggest that the highest discrepancy is about 0.0063 and is achieved at around 5600 K correlated color temperature (CCT). This study's results lay a firm path in customizing white-light LED modules that guarantee CRI and lumen output qualities.

This is an open access article under the [CC BY-SA](https://creativecommons.org/licenses/by-sa/4.0/) license.



Corresponding Author:

Anh Tuan Le,

Faculty of Electrical and Electronics Engineering,

Ton Duc Thang University,

Nguyen Huu Tho Street, Ho Chi Minh City, Vietnam.

Email: leanhtuan1@tdtu.edu.vn

1. INTRODUCTION

The white-light light-emitting diode (LED) is one of the most frequently used lighting methods in this industry. The fact that LEDs have so many remarkable traits such as high durability, good endurance against impacts, power saving, waste-free, and compact design allowing them to be used in many occasions from indoor lighting to lighting in tough condition as street lighting. The recent advancement in fast-switch brought even more attention as they are now also used in smart lighting, an auto lighting technology. To assess the lighting performance of LED, color rendering index (CRI), which is used to evaluate the LED light quality by comparing the light source from LED to the natural light or black-body radiation, is considered as a vital indicator. The result of CRI reflects the light quality of that LED, if the emission spectrum of phosphor in the LED resembling the broad continuous spectrum of black-body radiation, the CRI is high and so does the light quality [1-3]. For the construction of a white-light emitting structure with LED chips and phosphor, many approaches are suggested. However, the configuration containing one blue chip and a layer of yellow phosphor is the most popular method for cheap production cost [4, 5]. This configuration is discovered early on and the setting is not optimal, therefore, the CRI is still low although many efforts have been made to

enhance it such as using the chips emitting red and blue light with a yellow phosphor film. There are reports on instances that combination of phosphors and LED chips can adjust the emission spectrum to the desired value, thus, allowing the color quality and CRI to be set to the highest. The spectra of LED and phosphor with empirical and mathematical structures are analyzed to get the information that can help tuning the light color and changing CRI [6-8]. The obstacle with customized white LEDs that has adjustable correlated color temperatures (CCTs) is achieving high CRI while maintaining high luminous efficiency. This due to the package using a blue LED chip and two phosphor layers possibly attains great CRI values, yet the lumen output is inferior owing to the Stokes shift. On the other hand, though the package of single-layer phosphor with blue and red LED chips has both CRI and lumen efficacy, it is unable to adjust the color as the dual-layer phosphor structure does [9-12]. This leads to the solution of using the package with two LEDs and two phosphors for high CRI, yielded luminous flux and color tenability. In this research paper, based on Beer's law and linear conversion used for the subtle color difference production demands of white-light LEDs (WLED), a color design model is demonstrated. The WLED packages used for carried out the experiments are from yttrium aluminum garnet (YAG) and nitride-based phosphors in blue and red LEDs having good CRI and lumen efficacy. The different phosphor proportions and densities are used with silicone contains two types of LEDs to create the white LEDs. The obtained results show that the color design module suggested above is efficient and easy to fabricate.

2. PREPARATION AND SIMULATION

2.1. Preparation

$\text{CaGa}_2\text{S}_4:\text{Mn}^{2+}$ phosphor is used for the experiments in this study, the composition of $\text{CaGa}_2\text{S}_4:\text{Mn}^{2+}$ consists of 98% CaCO_3 , 2% MnCO_3 , and 200 (of Ga) Ga_2O_3 , and each component weighs 98 g, 2.3 g and 187 g, respectively [13-15]. To fabricate the red phosphor $\text{CaGa}_2\text{S}_4:\text{Mn}^{2+}$, there is a 5-step procedure that needs to be followed strictly to ensure the success and the quality of the product. The first step is to mix the ingredients by slurring in water, stop when the compound is mixed evenly. The next step is to leave the mixture in airy condition and let it dry. Then, grind the dehydrated mixture to get the powder. Next, put the powder from the previous step in open quartz boats, place it into a furnace with H_2S , at 900°C , and fire for 2 hours. When the firing process is done, take it out and begin to powderize. In the fourth step, place the compound in open quartz boats and put it through firing process again; this time fire at 800°C with N_2 loaded with CS_2 in 1 hour. The final step is storing the final product in a well-sealed container. The red phosphor $\text{CaGa}_2\text{S}_4:\text{Mn}^{2+}$ that come out of the process exhibits a deep red emission color and discharge the emission peak of 1.74 eV.

2.2. Simulation

The LightTools program is the essential tool to create the simulation of the LED and the Mie-theory is used to verify the accuracy of the results [16-19]. The simulation of the WLEDs with dual-layer phosphor can be proceeded after the parameters about the scattering properties of phosphor particles are gathered. Moreover, these information also assist the study of $\text{CaGa}_2\text{S}_4:\text{Mn}^{2+}$ phosphor's influence on WLEDs at a high correlated temperature of 5600 K. Figure 1 demonstrates how the compound of $\text{CaGa}_2\text{S}_4:\text{Mn}^{2+}$ and $\text{YAG}:\text{Ce}^{3+}$ phosphor is prepared to create the in-cup phosphor configuration of WLEDs. As can be seen, the order in which the phosphor layers are placed is $\text{CaGa}_2\text{S}_4:\text{Mn}^{2+}$ phosphor, the yellow phosphor $\text{YAG}:\text{Ce}^{3+}$, and the silicone glues. The WLEDs model illustrated in Figure 1 consists of a reflector cup, a silicone film, nine blue chips, and two phosphor layers. The parameters of the reflector that cover the chips are 2.07 mm depth, 8 mm bottom length, and 9.85 mm top surface length. Each of the 9 blue chips has the emission power of 1.16 W at 453 nm peak wavelength. The refractive index of $\text{CaGa}_2\text{S}_4:\text{Mn}^{2+}$ phosphor is 1.85 and $\text{YAG}:\text{Ce}^{3+}$ is 1.83. The concentration of $\text{YAG}:\text{Ce}^{3+}$ has to be changed appropriately to balance with the fluctuation of $\text{CaGa}_2\text{S}_4:\text{Mn}^{2+}$ concentration and keep the average CCTs.

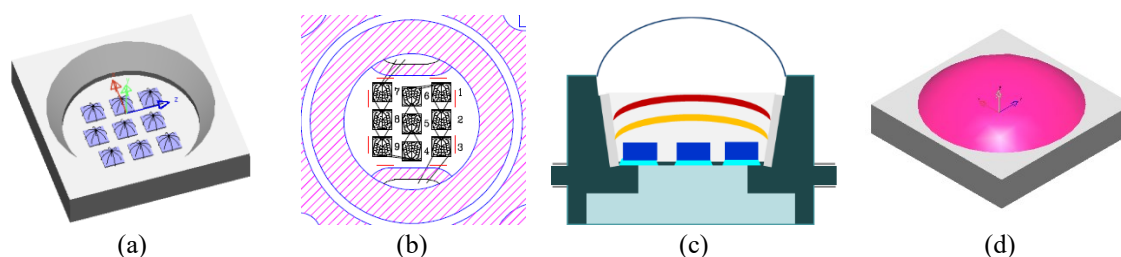


Figure 1. (a) 3D modelling, (b) bonding diagram, (c) model of pc-WLEDs cross-section, (d) illustration of WLEDs simulated from LightTools commercial software

3. RESULTS AND DISCUSSION

The changes to be made with YAG:Ce³⁺ phosphor to keep the average CCTs when CaGa₂S₄:Mn²⁺ phosphor increase are shown in Figure 2. In particular, when the concentration of CaGa₂S₄:Mn²⁺ is rising from 2-26% wt., the phosphor concentration of YAG:Ce³⁺ has to decrease accordingly to keep the average CCT, the tendency is unchanged with WLEDs at the color temperature of 5600K. The changes that are made based on these results also affect scattering and absorption properties, thus, leading to potential improvements in WLEDs color quality and light output. Furthermore, the performance of WLEDs is determined by CaGa₂S₄:Mn²⁺ phosphor, so choosing the concentration of this phosphor is very important.

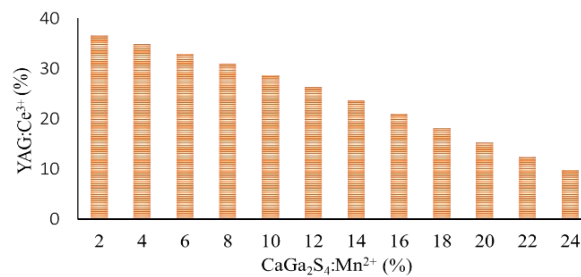


Figure 2. The balance between two phosphor concentrations to keep the average CCT

In Figure 3 are the effects of red phosphor CaGa₂S₄:Mn²⁺ in two different concentrations, 2% and 24%, on emission spectrum of WLEDs. The figure shows the luminous flux from WLED at 5600K ACCT, and the white light yielded from the spectral regions. The red line increases with the concentration of CaGa₂S₄:Mn²⁺ at three different regions: the most notable region is from 648–738 nm, and the other regions are from 420–480 nm and 500–640 nm. The increase in emission spectra from 420–480 nm boosts the scattered blue light. The results confirm the benefits of CaGa₂S₄:Mn²⁺ to the color quality of WLEDs having color temperature of 5600 K. This is an important finding because it helps the manufacturers choose the correct concentration to create WLEDs that suits their intention. A small disadvantage in WLEDs with high color quality that the manufacturers need to pay attention to is that the luminous flux of these WLEDs is reduced a bit.

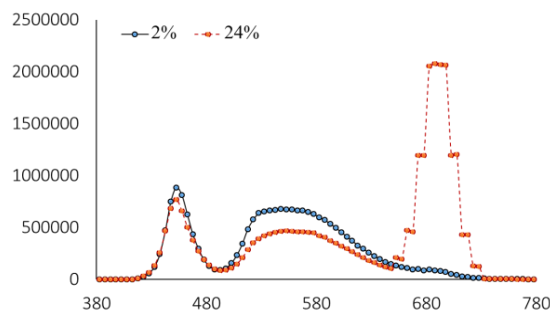


Figure 3. The emission spectra of WLEDs at 5600 K CCTs corresponding to CaGa₂S₄:Mn²⁺ concentration

The results from Figure 4 suggest that adding CaGa₂S₄:Mn²⁺ phosphor can increase CRI values for WLEDs. This is because of the absorbing characteristic of red phosphor CaGa₂S₄:Mn²⁺ that turns the absorbed blue light to red light. The red phosphor CaGa₂S₄:Mn²⁺ also absorbs yellow light; however, the absorbed blue light is still dominant due to the characteristic of the phosphor material. As a result, the red-light component in WLEDs increases when there is red phosphor CaGa₂S₄:Mn²⁺ in the package, which is beneficial to the CRI. Color rendering index is one of the indicators that can evaluate the quality of a WLED, the higher the CRI the better the quality of WLED and also the higher production cost. However, using CaGa₂S₄:Mn²⁺ phosphor can fix that problem because this is a low-cost method, and thus it allows WLEDs with CaGa₂S₄:Mn²⁺ phosphor to be used commonly. In recent years, CRI is not the most important index when evaluating the color quality of WLEDs because it is not a very in-depth indicator. Instead, the CQS is viewed as a more efficient and accurate parameter to express the performance of WLEDs. CQS with the ability to examine three elements of

WLEDs: color rendering index, viewer's preference, and color coordinates, is currently the most completed color quality index. Figure 5 shows the influence of $\text{CaGa}_2\text{S}_4:\text{Mn}^{2+}$ red phosphor on CQS. The results confirm that with dual phosphor layers WLEDs, the appearance of $\text{CaGa}_2\text{S}_4:\text{Mn}^{2+}$ phosphor enhances CQS significantly, which leads to the better color quality. Even though $\text{CaGa}_2\text{S}_4:\text{Mn}^{2+}$ phosphor can improve the color quality, the amount of reduced emitted light due to this phosphor cannot be ignored. The mathematical framework of the transmitted blue light and converted yellow light in the structure of two phosphor layers, a potential part that can promote the performance of WLEDs, is presented in the next part:

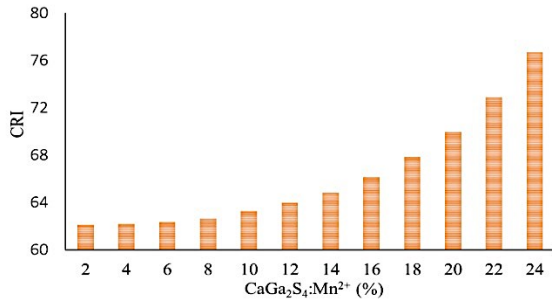


Figure 4. The color rendering index of WLEDs corresponding to $\text{CaGa}_2\text{S}_4:\text{Mn}^{2+}$ concentration

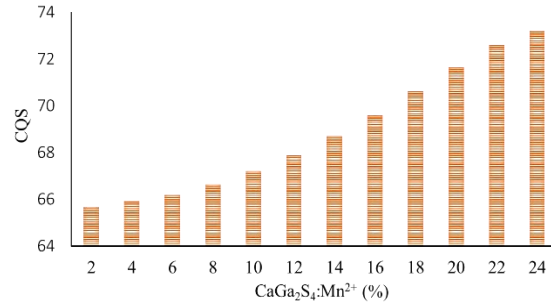


Figure 5. The color quality scale of WLEDs corresponding to $\text{CaGa}_2\text{S}_4:\text{Mn}^{2+}$ concentration

The Gaussian function is applied to model the asymmetrical SPD of monochrome [20, 21]:

$$P_\lambda = P_{opt} \frac{1}{\sigma\sqrt{2\pi}} \exp \left[-0.5 * \frac{(\lambda - \lambda_{peak})^2}{\sigma^2} \right] \quad (1)$$

In (1), σ is a parameter depending on the peak wavelength λ_{peak} , and the computation of FWHM $\Delta\lambda$ can be presented as:

$$\sigma = \frac{\lambda^2_{peak} \Delta E}{2hc\sqrt{2} \ln 2} = \frac{\lambda^2_{peak} \left(\frac{hc}{\lambda_1} - \frac{hc}{\lambda_2} \right)}{2hc\sqrt{2} \ln 2} = \frac{\lambda^2_{peak} \left(\frac{hc\Delta\lambda}{\lambda_1\lambda_2} \right)}{2hc\sqrt{2} \ln 2} \quad (2)$$

The SPD of a WLED utilizing yellow YAG phosphor and blue chip can hypothetically be viewed as the aggregate of the spectra of yellow and blue rays. Practically speaking, nonetheless, the supposed yellow phosphor radiates light in both yellow and green spectra (as demonstrated from the deliberate spectra in Figures 1 and 2). In the event that both yellow and blue ranges are picked, the contrast between the essentially estimated SPD and twofold shading (yellow and blue shading) range model can be spoken to by a green range. In this manner, so as to speak to the down to earth circumstance, a green range can be added to the twofold range model, bringing about the accompanying investigative tri-spectrum (B–G–Y) module represented by (3) and finally altered by (4).

$$P_\lambda = P_{opt_b} \frac{1}{\sigma_b\sqrt{2\pi}} \exp \left[-0.5 * \frac{(\lambda - \lambda_{peak_b})^2}{\sigma_b^2} \right] + P_{opt_g} \frac{1}{\sigma_g\sqrt{2\pi}} \exp \left[-0.5 * \frac{(\lambda - \lambda_{peak_g})^2}{\sigma_g^2} \right] + P_{opt_y} \frac{1}{\sigma_y\sqrt{2\pi}} \exp \left[-0.5 * \frac{(\lambda - \lambda_{peak_y})^2}{\sigma_y^2} \right] \quad (3)$$

$$P_\lambda = \eta_b P_{opt_total} \frac{1}{\sigma_b\sqrt{2\pi}} \exp \left[-0.5 * \frac{(\lambda - \lambda_{peak_b})^2}{\sigma_b^2} \right] + \eta_g P_{opt_total} \frac{1}{\sigma_g\sqrt{2\pi}} \exp \left[-0.5 * \frac{(\lambda - \lambda_{peak_g})^2}{\sigma_g^2} \right] + \eta_y P_{opt_total} \frac{1}{\sigma_y\sqrt{2\pi}} \exp \left[-0.5 * \frac{(\lambda - \lambda_{peak_y})^2}{\sigma_y^2} \right] \quad (4)$$

P_λ represents the spectral power distribution (SPD) (mW/nm). h , c and λ are the constant of Planck (J.s), the speed of light ($\text{m} \cdot \text{s}^{-1}$), and the wavelength (nm), respectively. The optical power (W) is indicated by P_{opt} , and the peak wavelength is expressed as λ_{peak} (nm). $\Delta\lambda$ shows the full-width at half-maximum (FWHM) (nm), while η is the symbol of ratio of specific spectra to white spectrum, dimensionless. The parameters P_{opt_b} , P_{opt_g} , P_{opt_y} , and P_{opt_total} presents the optical power (W) for the blue, green, yellow, and white spectra, in turn.

Meanwhile, λ_{peak_b} , λ_{peak_g} , and λ_{peak_y} are viewed as the peak wavelengths (nm) for the blue, green, and yellow spectra, respectively. σ_b , σ_g , and σ_y are respectively known as FWHM-related coefficients (nm) for the blue, green, and yellow spectra. η_b , η_g , and η_y indicate the ratios of blue–green–yellow (B–G–Y) spectra to white spectrum, respectively, dimensionless; and λ_1 , λ_2 are the wavelengths at half of the peak intensity.

Hence, it is possible to express the modeled SPD of the phosphor-coated WLED as a tricolor spectrum, and we can consider it as an extended Gaussian model. In addition, through the application of Mie-scattering theory, the analysis of $\text{CaGa}_2\text{S}_4:\text{Mn}^{2+}$ scattering, and also the computation of scattering cross section C_{sca} for spherical particles were carried out [22, 23]. Besides that, the Lambert-Beer law is used for calculating the transmitted light power [24, 25]:

$$I = I_0 \exp(-\mu_{ext}L) \quad (5)$$

I_0 represents the incident light power, while L indicates the thickness of the phosphor film (mm). μ_{ext} in this formula is the extinction coefficient that can be calculated through this equation: $\mu_{ext} = N_r \cdot C_{ext}$, with N_r is the number density distribution of particles (mm^{-3}), and C_{ext} (mm^2) presents the extinction cross-section of phosphor particles.

By applying (5), the outcome shows that using dual-layer remote phosphor structure can create a much better luminous flux than using single-layer phosphor structure. Therefore, this confirms the usefulness of dual-layer phosphor structure to the improvement of luminous flux in WLEDs. The optical performance of dual-layer phosphor structure WLEDs with red phosphor $\text{CaGa}_2\text{S}_4:\text{Mn}^{2+}$ is greatly influenced by the concentration of $\text{CaGa}_2\text{S}_4:\text{Mn}^{2+}$. In particular, the extinction coefficient μ_{ext} demonstrated in the Lambert-Beer law and concentration of $\text{CaGa}_2\text{S}_4:\text{Mn}^{2+}$ increase together. However, the light emission energy increases in inverse direction to the extinction coefficient μ_{ext} . As a result, the luminous flux of WLEDs is reduced when increasing both phosphor layers thickness by adding more $\text{CaGa}_2\text{S}_4:\text{Mn}^{2+}$. Figure 6 illustrates this statement by presenting decreasing luminous fluxes in all CCTs when the concentration of $\text{CaGa}_2\text{S}_4:\text{Mn}^{2+}$ moves to 26%. In hindsight, using dual-layer phosphor structure with red phosphor $\text{CaGa}_2\text{S}_4:\text{Mn}^{2+}$ already created a much better luminous flux than the single-layer phosphor one, not to mention the benefits that $\text{CaGa}_2\text{S}_4:\text{Mn}^{2+}$ has on the development of CRI and CQS. Therefore, a minor decrease in luminous flux is acceptable, considering how the advantages outweigh the disadvantage. The most suitable concentration setting depends on the manufacturer choices, as the optimal concentration of $\text{CaGa}_2\text{S}_4:\text{Mn}^{2+}$ is the one that can adapt to their demands of quality in WLEDs mass production.

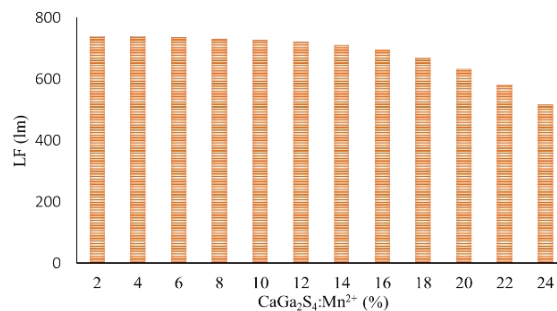


Figure 6. The luminous flux of WLEDs as a function of $\text{CaGa}_2\text{S}_4:\text{Mn}^{2+}$ concentration

4. CONCLUSION

This research comes up with an effective technique through experimental results to create WLEDs with high CRI and luminous efficacy, and allow constant changes to the spectrum of the target. From Lambert Beer law and linear conversion, a color design model that can change the white light from LEDs to match the need of the manufacturers was created. The spectrum of the simulation and the measured one are compatible with each other, the biggest gap between CIE 1931 simulation and the measured is about 0.0063 near the CCT of 5600 K. This trait is helpful for the formation and application of the color design model.

REFERENCES

- [1] S. P. Ying, H. K. Fu, H. H. Hsieh, K. Y. Hsieh, "Color design model of high color rendering index white-light LED module," *Applied Optics*, vol. 56, no. 14, pp. 4045-4051, 2017.

- [2] L. Wang, X. Zhang, Z. D. Hao, Y. S. Luo, X. J. Wang, J. H. Zhang, "Enriching red emission of $\text{Y}_3\text{Al}_5\text{O}_{12}:\text{Ce}^{3+}$ by codoping Pr^{3+} and Cr^{3+} for improving color rendering of white LEDs," *Optics Express*, vol. 18, no. 24, pp. 25177-25182, 2010.
- [3] V. V. Bakhmet'ev, V. V. Malygin, L. A. Lebedev, M. V. Keskinova, M. M. Sychev, "Synthesis of finely dispersed $\text{NaBaPO}_4:\text{Eu}^{2+}$ phosphors and structural investigation of their centers of luminescence," *Journal of Optical Technology*, vol. 84, no. 9, pp. 642-646, 2017.
- [4] H. F. Sijbom, R. Verstraete, J. J. Joos, D. Poelman, P. F. Smet, " $\text{K}_2\text{SiF}_6:\text{Mn}^{4+}$ as a red phosphor for displays and warm-white LEDs: a review of properties and perspectives," *Optical Materials Express*, vol. 7, no. 9, pp. 3332-3365, 2017.
- [5] S. H. Kim, Y. H. Song, S. R. Jeon, et al., "Enhanced luminous efficacy in phosphor-converted white vertical light-emitting diodes using low index layer," *Optics Express*, vol. 21, no. 5, pp. 6353-6359, 2013.
- [6] F. Z. Zhang, H. S. Xu, Z. Wang, "Optimizing spectral compositions of multichannel LED light sources by IES color fidelity index and luminous efficacy of radiation," *Applied Optics*, vol. 56, no. 7, pp. 1962-1971, 2017.
- [7] D. Dinakaran, C. Gossler, C. Mounir, et al., "Phosphor-based light conversion for miniaturized optical tools," *Applied Optics*, vol. 56, no. 13, pp. 3654-3659, 2017.
- [8] Z. Wang, S. Lou, P. Li, Z. Lian, "Single-phase tunable white-light-emitting $\text{Sr}_3\text{La}(\text{PO}_4)_3:\text{Eu}^{2+}, \text{Mn}^{2+}$ phosphor for white LEDs," *Applied Optics*, vol. 56, no. 4, pp. 1167-1172, 2017.
- [9] Y. Peng, Y. Mou, X. Guo, et al., "Flexible fabrication of a patterned red phosphor layer on a $\text{YAG}:\text{Ce}^{3+}$ phosphor-in-glass for high-power WLEDs," *Optical Materials Express*, vol. 8, no. 3, pp. 605-614, 2018.
- [10] H. Lee, S. Kim, J. Heo, W. J. Chung, "Phosphor-in-glass with Nd-doped glass for a white LED with a wide color gamut," *Optics Letters*, vol. 43, no. 4, pp. 627-630, 2018.
- [11] C. N. Li, H. B. Rao, W. Zhang, C. Y. Zhou, Q. Zhang, K. Zhang, "Self-Adaptive Conformal-Remote Phosphor Coating of Phosphor-Converted White Light Emitting Diodes," *Journal of Display Technology*, vol. 12, no. 9, pp. 946-950, 2016.
- [12] N. D. Q. Anh, P. X. Le, H. Y. Lee, "Selection of a Remote Phosphor Configuration to Enhance the Color Quality of White LEDs," *Current Optics and Photonics*, vol. 3, no. 1, pp. 78-85, 2019.
- [13] Z. T. Li, H. Y. Wang, B. H. Yu, X. R. Ding, Y. Tang, "High-efficiency LED COB device combined diced V-shaped pattern and remote phosphor," *Chinese Optics Letters*, vol. 15, no. 4, 2017.
- [14] C. F. Lai, Y. C. Lee, C. T. Kuo, "Saving Phosphor by 150% and Producing High Color-Rendering Index Candlelight LEDs Containing Composite Photonic Crystals," *Journal of Lightwave Technology*, vol. 32, no. 10, pp. 1930-1935, 2014.
- [15] K. A. G. Smet, P. Hanselaer, "Impact of cross-regional differences on color rendition evaluation of white light sources," *Optics Express*, vol. 23, no. 23, pp. 30216-30226, 2015.
- [16] J. H. Oh, S. J. Yang, Y. G. Sung, Y. R. Do, "Excellent color rendering indexes of multi-package white LEDs," *Optics Express*, vol. 20, no. 18, pp. 20276-20285, 2012.
- [17] Y. Peng, X. Guo, R. X. Li, H. Cheng, M. X. Chen, "Thermally stable WLEDs with excellent luminous properties by screen-printing a patterned phosphor glass layer on a microstructured glass plate," *Applied Optics*, vol. 56, no. 12, pp. 3270-3276, 2017.
- [18] H. L. Shi, C. Zhu, J. Q. Huang, J. Chen, D. C. Chen, W. C. Wang, et al., "Luminescence properties of $\text{YAG}:\text{Ce}, \text{Gd}$ phosphors synthesized under vacuum condition and their white LED performances," *Optical Materials Express*, vol. 4, no. 4, pp. 649-655, 2014.
- [19] C. H. Huang, T. W. Kuo, T. M. Chen, "Thermally stable green $\text{Ba}_3\text{Y}(\text{PO}_4)_3:\text{Ce}^{3+}, \text{Tb}^{3+}$ and red $\text{Ca}_3\text{Y}(\text{AlO})_3(\text{BO}_3)_4:\text{Eu}^{3+}$ phosphors for white-light fluorescent lamps," *Optics Express*, vol. 19, no. 101, 2011.
- [20] V. Heikkinen, I. Kassamakov, T. Paulin, A. Nolvi, E. Hæggröm, "Stroboscopic scanning white light interferometry at 2.7 MHz with 1.6 μm coherence length using a non-phosphor LED source," *Optics Express*, vol. 21, no. 5, pp. 5247-5254, 2013.
- [21] F. Che, L. Wu, B. Hussain, X. Li, C. P. Yue, "A Fully Integrated IEEE 802.15.7 Visible Light Communication Transmitter with On-Chip 8-W 85% Efficiency Boost LED Driver," *Journal of Lightwave Technology*, vol. 34, no. 10, pp. 2419-2430, 2016.
- [22] N. Narendran, Y. Gu, "Life of LED-Based White Light Sources," *Journal of Display Technology*, vol. 1, no. 1, pp. 167-171, 2005.
- [23] H. Segawa, N. Hirotsuki, "Europium-doped SiAlON and borosilicate glass composites for white light-emitting diode," *Applied Optics*, vol. 54, no. 29, pp. 8727-8730, 2015.
- [24] W. G. Bi, X. F. Jiang, H. Q. Wu, F. Zhao, "Improved efficacy of warm-white light-emitting diode luminaires," *Applied Optics*, vol. 54, no. 6, pp. 1320-1325, 2015.
- [25] G. Zhang, K. Ding, G. He, P. Zhong, "Spectral optimization of color temperature tunable white LEDs with red LEDs instead of phosphor for an excellent IES color fidelity index," *OSA Continuum*, vol. 2, no. 4, pp. 1056-1064, 2019.